Supramolecular Organic Frameworks with Ultralong Phosphorescence via Breaking π-Conjugated Structures

Wei Yao , Chaoqun Ma , Huili Ma , Lishun Fu , Song Lu , Anqi Lv , Suzhi Cai , Xiaochun Hang , Manjeet Singh , Huifang Shi , Zhongfu An , Wei Huang

PII: S2666-5425(20)30007-2
DOI: https://doi.org/10.1016/j.giant.2020.100007
Reference: GIANT 100007

To appear in: *Giant*

Received date: 21 March 2020
Revised date: 25 April 2020
Accepted date: 5 May 2020

Please cite this article as: Wei Yao , Chaoqun Ma , Huili Ma , Lishun Fu , Song Lu , Anqi Lv , Suzhi Cai , Xiaochun Hang , Manjeet Singh , Huifang Shi , Zhongfu An , Wei Huang , Supramolecular Organic Frameworks with Ultralong Phosphorescence via Breaking π-Conjugated Structures, *Giant* (2020), doi: https://doi.org/10.1016/j.giant.2020.100007

Supramolecular Organic Frameworks with Ultralong Phosphorescence via Breaking π-Conjugated Structures

Wei Yao,[†a] Chaoqun Ma,[†a] Huili Ma,[a] Lishun Fu,[a] Song Lu,[a] Anqi Lv,[a] Suzhi Cai,[a] Xiaochun Hang,[a] Manjeet Singh,[a] Huifang Shi,[*a] Zhongfu An[*a] and Wei Huang[*a,b]

[a] Key Laboratory of Flexible Electronics (KLOFE) & Institute of Advanced Materials (IAM) Nanjing Tech University (NanjingTech), 30 South Puzhu Road, Nanjing 211816, China. *E-mail: iamhfshi@njtech.edu.cn, iamzfan@njtech.edu.cn[b] Frontiers Science Center for Flexible Electronics (FSCFE), Shaanxi Institute of Flexible Electronics (SIFE) & Shaanxi Institute of Biomedical Materials and Engineering (SIBME), Northwestern Polytechnical University (NPU), 127 West Youyi Road, Xi'an 710072, China. E-mail: provost@nwpu.edu.cn

† These authors contributed equally.

Abstract

Development of crystalline porous materials with luminescent properties have gradually attracted attention for their potential applications in drug delivery, bioimaging, photoelectronic and so on. To date, it is a formidable challenge to rationally design porous phosphorescent materials. Herein, we have reported a chemical strategy of breaking π-conjugated structures of phosphorescent molecules by alkyl chain to achieve supramolecular organic framework (SOFs) with visible ultralong phosphorescence (lifetime > 600 ms). The molecules having broken π-conjugation by flexible alkyl chain will be beneficial to produce short-range π-π stacking for forming luminescent SOFs. Effective π-π stacking between chromophores stabilized triplet excitons to contribute to ultra-long phosphorescence. This work demonstrates a new approach to design porus materials with ultralong phosphorescence and will expand the potential applications of organic phosphorescent crystals with diverse pores.

Keywords

Supramolecular organic frameworks; Ultralong organic phosphorescence; π-π stacking; Persistent luminescence

1. Introduction

Organic porous luminescent materials, mainly including metal organic frameworks (MOFs) [1-3], covalent organic frameworks (COFs) [4,5] and supramolecular organic framework (SOFs) [6,7], have triggered considerable interests due to their potential applications in sensing [1,8-12], drug delivery [13,14], bioimaging [15], lighting [16-18] and so on [19-22], which mainly emit fluorescence. As compared to fluorescence, phosphorescence, especially ultralong phosphorescence, shows long emission lifetime and high exciton utilization [23-26], which makes phosphorescent materials as good candidates in bioimaging [27,28], data encryption [29,30], sensors [31], etc [32-36]. For example, taking advantage of the long-lived emission, the time-gated optical techniques, such as time-resolved emission spectra and florescence lifetime imaging microscopy, can be utilized to eliminate the inference from the background florescence, and thus enhancing the signal-to-noise ratio greatly in biosensing or bioimaging [28]. Therefore, the development of porous materials with phosphorescence is of great significance. For MOFs, both fluorescence and phosphorescence could be realized due to the facilitated spin-orbital coupling (SOC) by metal elements and aromatic ligands [37,38]. However, scarce resources and high biotoxicity of metals [39], promote researchers to divert their attention towards COFs and SOFs. Nevertheless, due to the inefficient SOC and rapid non-radiative decay of triplet excitons, it is difficult to achieve phosphorescence in COFs and SOFs. Although the COFs have high chemical and thermal stability, the harsh preparation conditions, uncertain structural characterization and low crystallinity [39,40] make construction of phosphorescent COFs more challenging. In view of the mild preparation conditions, easy purification and recyclability of the SOFs, we reason that it is more practicable to develop metal-free SOFs with phosphorescent emission, or even ultralong organic phosphorescence (UOP).

Traditional SOFs without phosphorescence can be constructed by directional hydrogen bonding or host-guest molecular system and so on, having hydrogen bond donor and acceptor sites to form strong hydrogen bonding for generating pores, such as carboxyl group, amide group, pyridine and so on [41-43]. We believe that molecules with groups that can simultaneously form hydrogen bonds and produce phosphorescence are favourable to construct SOFs with UOP. Recently, our group has reported the first carbazole derivative that showed three types of hydrogen-bonded organic aromatic frameworks with the longest phosphorescence life-time of 79.8 ms by the short-range π-π stacking [44]. Inspired by this concept, we deduced that the control of π-π stacking of UOP crystals plays an important role in the construction of SOF structures.

The typical phosphorescent chromophores, DMCz and DPCz exhibited yellow ultralong phosphorescence due to the perfect H-aggregation of coplanar molecules with long-range π-π stacking (Fig. 1a) [29,45]. To break the planarity as well as long-large π-conjugated structures into short-range π-π stacking to construct HOFs, a flexible alkyl chain with appropriate length is introduced in the typical phosphorescent chromophores, because of their effects on twisting molecular configuration and controlling molecular steric hindrance [46,47].

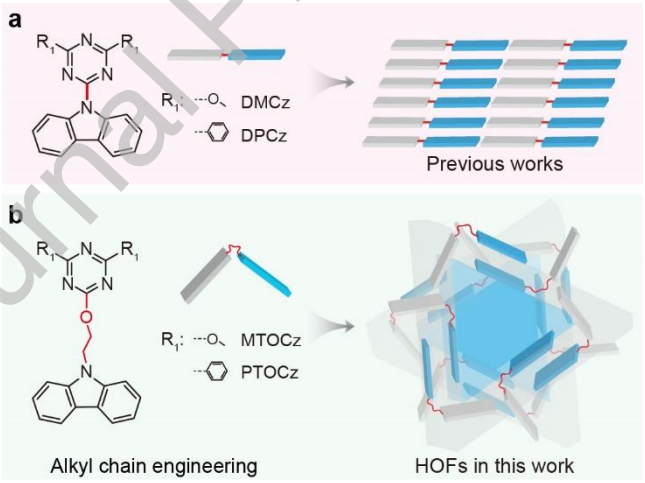

Fig. 1. (a) Typical ultralong phosphorescent molecules and schematic representation of their molecular stacking in crystal. (b) Target molecules for the construction of supramolecular organic framework (SOFs) and schematic diagram of the SOFs.

As expected, we have constructed metal-free SOFs with ultralong phosphorescence by breaking large π-conjugated structures into two parts using a flexible alkyl chain (Fig. 1b). The porosity of SOFs has been generated by the combination of short-range π-π stacking and the introduced flexible alkyl chains. Both SOFs having driving forces (weak polar π-π and C-H…π interactions), remain their ultralong phosphorescence property, with lifetime over 600 ms. We have achieved the longest phosphorescence lifetime in the reported SOFs so far and provided a feasible strategy for the construction of SOFs with improved phosphorescence lifetime.

2. Material and methods

2.1 Synthesis and Characterizations

To verify our hypothesis, we designed and synthesized a pair of SOFs 9-(2-((4,6-diphenyl-1,3,5-triazin-2-yl)oxy)ethyl)-9H-carbazole (PTOCz) and 9-(2-((4,6-dimethoxy-1,3,5-triazin-2-yl)oxy)ethyl)-9H-carbazole (MTOCz) via covalently attached carbazole units with triazine core by alkyl alcohol, respectively (Scheme 1). The chemical structures and purity of products were fully characterized by NMR spectroscopy (Fig. S1-S5), high resolution mass spectra, single-crystal and powder X-ray diffraction (Fig. S6) as well as high performance liquid chromatography HPLC (Fig. S7).

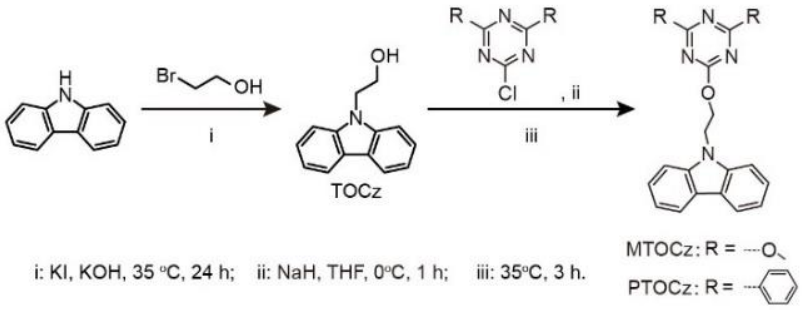

Scheme 1. Synthetic routes of the target molecules.

2.2 Synthesis of PTOCz and MTOCz compounds

2-(9H-carbazol-9-yl)ethan-1-ol (TOCz): Dissolved carbazole (1 g, 5.97 mmol), potassium iodide(0.49 g, 2.98 mmol) and potassium hydroxide (2.01 g, 35.82 mmol) with dimethylformamide (DMF) (20-30 mL) in a 100 mL round-bottom flask equipped with a stirring bar, then 2-bromoethan-1-ol (0.37 g, 2.98 mmol) was injected into the round-bottom flask slowly and stirred the mixture at 35oC for 3 h. ^{1}H NMR (400 MHz, $CDCl_3$): δ 8.13 (d , 2H), 7.54-7.45 (m, 4H), 7.32-7.27 (m, 2H), 4.48 (t, 2H), 4.05 (q, 2H).

9-(2-((4,6-diphenyl-1,3,5-triazin-2-yl)oxy)ethyl)-9H-carbazole (PTOCz): Mixed sodium hydride (0.087 g, 2.13 mmol) and 2-(9H-carbazol-9-yl)ethan-1-ol (0.3 g, 1.42 mmol) were added in a 10 mL round-bottom flask equipped with a stirring bar, then dry tetrahydrofuran (THF) (2-3 mL) was injected into the round-bottom flask and the mixture was stirred at room temperature for 0.5 h. 2-chloro-4,6-diphenyl-1,3,5-triazine (0.38 g, 1.42 mmol) was dissolved with dry THF (35 mL) in a 100 mL round-bottom flask equipped with a stirring bar. Above mixture solution was added in 2-chloro-4,6-diphenyl-1,3,5-triazine solution dropwise at 35 °C. After stirring at 35 °C for 10 h, THF was removed by rotary evaporation. Then extracted it with CH_2Cl_2 and water for three times, the organic layers were collected and dried over sodium sulfate. Solvent CH_2Cl_2 was removed by rotary evaporation and the product was purified by flash column chromatography to give white powder. ^{1}H NMR (400 MHz, $CDCl_3$): δ 8.55 (d, 4H), 8.08 (d, 2H), 7.65-7.48 (m, 10H), 7.25 (d, 2H), 5.04 (t, 2H), 4.86 (t, 2H). ^{13}C NMR (100 MHz, CDCl3): δ 173.67, 171.20, 140.34, 135.38, 132.80, 129.08, 128.59, 125.93, 123.14, 120.50, 119.41, 108.56, 64.31, 41.71. LCMS-TOF (m/z): calcd for $C_{29}H_{22}N_4O_1$ 442.52. Found: 443.19147.

9-(2-((4,6-dimethoxy-1,3,5-triazin-2-yl)oxy)ethyl)-9H-carbazole (MTOCz): Following the similar synthetic procedure of PTOCz. 2-(9H-carbazol-9-yl)ethan-1-ol (0.3 g, 1.42 mmol), sodium hydride (0.087 g, 2.13 mmol) and 2-chloro-4,6-dimethoxy-1,3,5-triazine (0.38 g, 1.42 mmol) were reacted to produce 0.1 g white powder. ^{1}H NMR (400 MHz, $CDCl_3$): δ 8.07 (d, 2H), 7.51-7.44 (m, 4H), 7.26-7.21 (m, 2H), 4.85-4.65 (m, 4H), 3.90 (s, 6H).^{13}C NMR (100 MHz, CDCl3): δ 173.44, 172.78, 140.33, 125.89, 123.08, 120.41, 119.36, 108.58, 65.22, 55.33, 41.71. LCMS-TOF (m/z): calcd for $C_{19}H_{18}N_4O_3$ 350.38. Found:351.14490.

2.3 The preparation of crystals:

Prepared powders of PTOCz (10 mg) were dissolved in CH_2CH_2 (1 mL) and let stand until no solid can be observed by naked eyes. Then hexane (1-2 mL) was slowly added into above solution as a poor solvent. The mixture was kept in an undisturbed environment about 25°C for two days for crystal formation and rod-like crystals were obtained. The narrow sheet MTOCz crystals were cultivated under the same conditions as PTOCz. As shown in Figure S8, it is found that both PTOCz and MTOCz crystals show rod-like crystals.

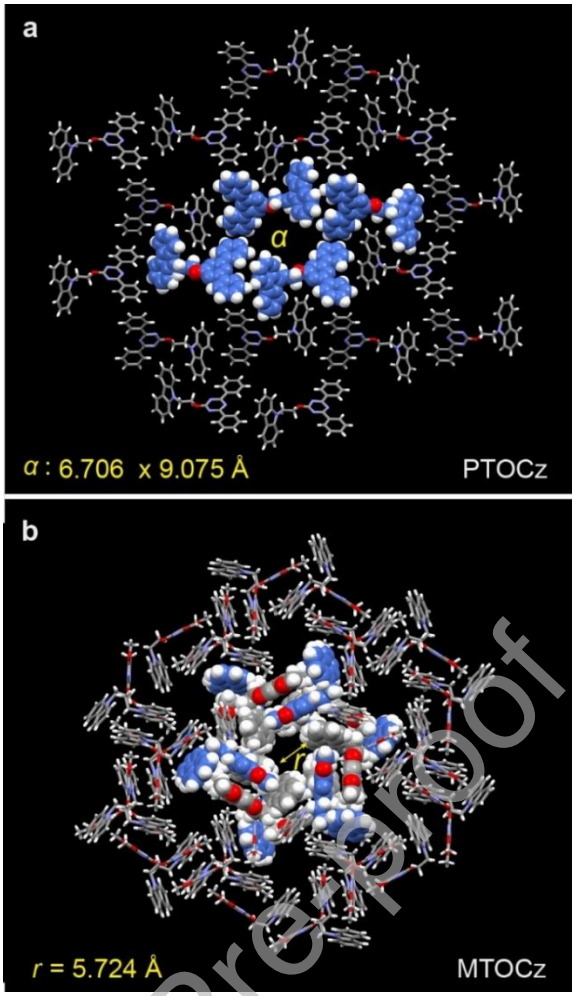

Fig. 2. Molecular stacking of (a) PTOCz and (b) MTOCz in crystal viewed from c axis.

3. Results and discussion

3.1 Porous Properties.

Both molecules (DPCz and DMCz) are densely packed in their crystals due to the planar structures (Fig. 1a, S9), which makes them difficult to generate porosity in crystalline state. In this work, the planar configurations of the selected molecules have been broken by the introduction of flexible oxoalkyl chains between the triazine and the carbazole cores. As shown in Fig. 1b, the triazine and the carbazole cores have retained their planar configurations, but they are oriented almost perpendicular to each other to form a three-dimensional (3D) structure with empty space (Fig. S10). The dihedral angles between triazine and carbazole cores are different in PTOCz and MTOCz, and they were found to be 68.48^{o} and 82.95^{o}, respectively. We rationalized that the alkoxyl chain with appropriate length could pro-vide enough distance between two planar parts to eliminate steric hindrance as well as planarity of their original molecules, which further develop new cubical structures. Various intermolecular interactions along with π-π stacking have tightly fixed the above cubical structures, which plays a critical role to generate ordered pores.

The crystal packing analysis shows that PTOCz crystal has rectangular pores with the dimension of 6.706 X 9.075 Å around with four molecules in different layers (Fig. 2a) and MTOCz crystal has hexagonal pores with a diameter of 5.724 Å (Fig. 2b) around with six molecules in different layers. The hexagonal shape of the MTOCz pore can be clearly seen from Fig. S11, where three pairs of interlocked molecules in the same layer form a triangle and such two triangles of two different layers are staggered and arranged in a hexagonal shape.

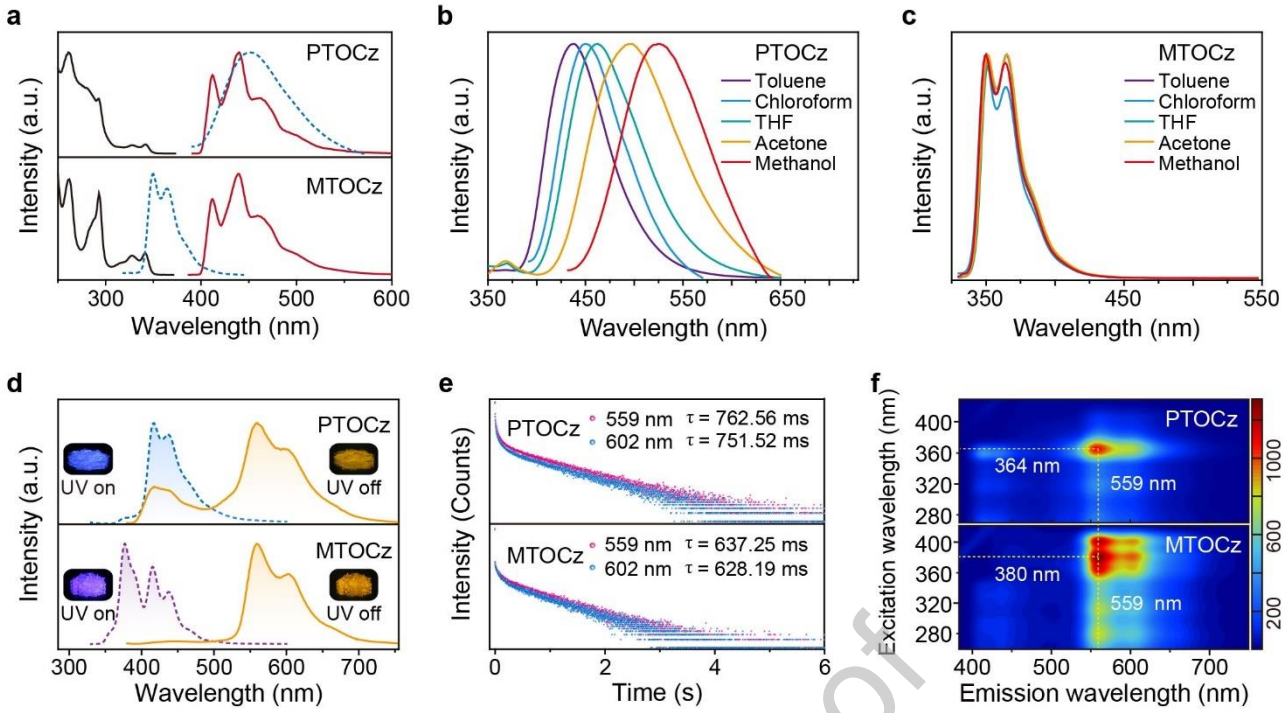

Fig. 3. Photophysical properties of PTOCz and MTOCz molecules. (a) Absorption (black lines) and steady-state photoluminescence (PL, blue dotted lines) spectra in $CHCl_3$ solution (1×10^{-5} M) under ambient conditions, as well as phosphorescence (red lines) spectra of PTOCz and MTOCz in solution (2-methyl tetrahydrofuran, 1×10^{-5} M) at 77 K. (b), (c) PL spectra of PTOCz and MTOCz in different solvents, respectively. (d) Steady-state PL (blue or purple lines) and phosphorescence (orange lines) spectra of crystalline PTOCz and MTOCz under ambient conditions. The phosphorescence spectra were collected with a delay time of 8 ms. Insets show photographs of PTOCz and MTOCz crystals under 365 nm UV light on (left) and off (right), respectively. (e) Lifetime decay profiles of PTOCz and MTOCz crystals at different emission peaks under ambient conditions. (f) Excitation-phosphorescence mapping of PTOCz and MTOCz crystals under ambient conditions.

3.2 Photophysical Properties of PTOCz and MTOCz.

Subsequently, we have systematically investigated the photophysical properties of PTOCz and MTOCz in solution as well as in crystalline states. As shown in Fig. 3a, PTOCz and MTOCz displayed absorbance peaks at 262, 293, 328 and 342 nm in dilute $CHCl_3$ solution, which is similar to their corresponding molecular structures, but with different absorption intensities.

The steady-state photoluminescence (PL) spectra of both compounds have also recorded in dilute $CHCl_3$ solution under ambient conditions, MTOCz showed well-split emission peaks at 310 and 330 nm, which was attributed to emission of fine structure in local excited (LE). In comparison to MTOCz, PTOCz exhibited a broad and redshifted emission band around 450 nm, which may be due to the charge transfer (CT) emission.[48] In order to verify the surmise, we have conducted a series of spectra of PTOCz and MTOCz in various solvents with different polarity. As shown in Fig. 3b, with increasing of polarity of solvent, the PL peaks of PTOCz were gradually redshifted from 437 to 525 nm according to the intrinsic characteristics of CT emission[49,50]. In contrast, the PL spectra of MTOCz solutions did not show any shift (Fig. 3c) on in-creasing polarity of the solvent. Above results demonstrated that PL emission of MTOCz was ascribed to LE emission.

Additionally, we have also performed phosphorescence spectroscopy of PTOCz and MTOCz in dilute 2-methyltetrahydrofuran solution at 77 K, showed similar emission peaks at 413, 440 and 462 nm, which demonstrated the single molecular phosphorescent emission (Fig. 3a). As expected, both SOFs have obvious UOP under ambient conditions. In crystalline state, PTOCz showed blue emission at 437 nm (τ= 16.46 ns) under 365 nm excitation; while MTOCz exhibited purple emission with the emission peaks at 377 nm (τ= 3.74 ns), 416 nm (τ= 17.56 ns) and 437 nm (τ = 17.76 ns) (Fig. 3d and S12, Table S1). It is attributed to the different molecular packing of PTOCz and MTOCz crystals. After removing the exciting light source, orange ultralong luminescence from both SOFs can be observed by naked eyes lasting for several seconds. For PTOCz, its phosphorescent spectrum with a delay time of 8 ms under ambient conditions exhibited obvious peaks at 418, 559 and 602 nm with ultralong lifetimes of 607.56 ms (Fig. S11a), 762.56 and 751.52 ms, respectively (Fig. 3d and e, Table S1). Similarly, MTOCz crystal also showed phosphorescent spectrum with emission peaks at 443 nm (τ = 137.04 ms), 559 nm (τ = 637.25 ms) and 602 nm (τ = 628.19 ms). The quantum yields of the phosphorescence for PTOCz and MTOCz are 0.33% and 0.057%, respectively (Table S2). Among these, emission bands at around 418 nm of PTOCz and 443 nm of MTOCz in their phosphorescent spectra with ultralong life-times belong to triplet-triplet annihilation (TTA) emission due to the larger π-π overlaps of triazine units and carbazole groups between their neighbouring molecules [51,52], respectively (Fig. S13). The emission peaks at 559 and 602 nm appeared in their phosphorescent

spectra belonged to phosphorescent emission. In addition, we found that the phosphorescent emission of PTOCz and MTOCz crystals under ambient conditions were different from those in dilute solution at 77 K. It indicates that the UOP of these SOFs were originally generated from aggregated molecules rather than the single molecular state. Notably, the UOP lifetimes of two SOFs are pretty longer than the previous work [44]. From Fig. S14, the UOP intensities of the HOF crystals have decreased in oxygen obviously compared to that in vacuum. These results demonstrate that the SOFs in this work have potential as oxygen sensors. Additionally, from the excitation-phosphorescence mapping ranged from 280 to 400 nm, UOP of PTOCz and MTOCz in crystal can be optimally excited by 360 and 380 nm, respectively.

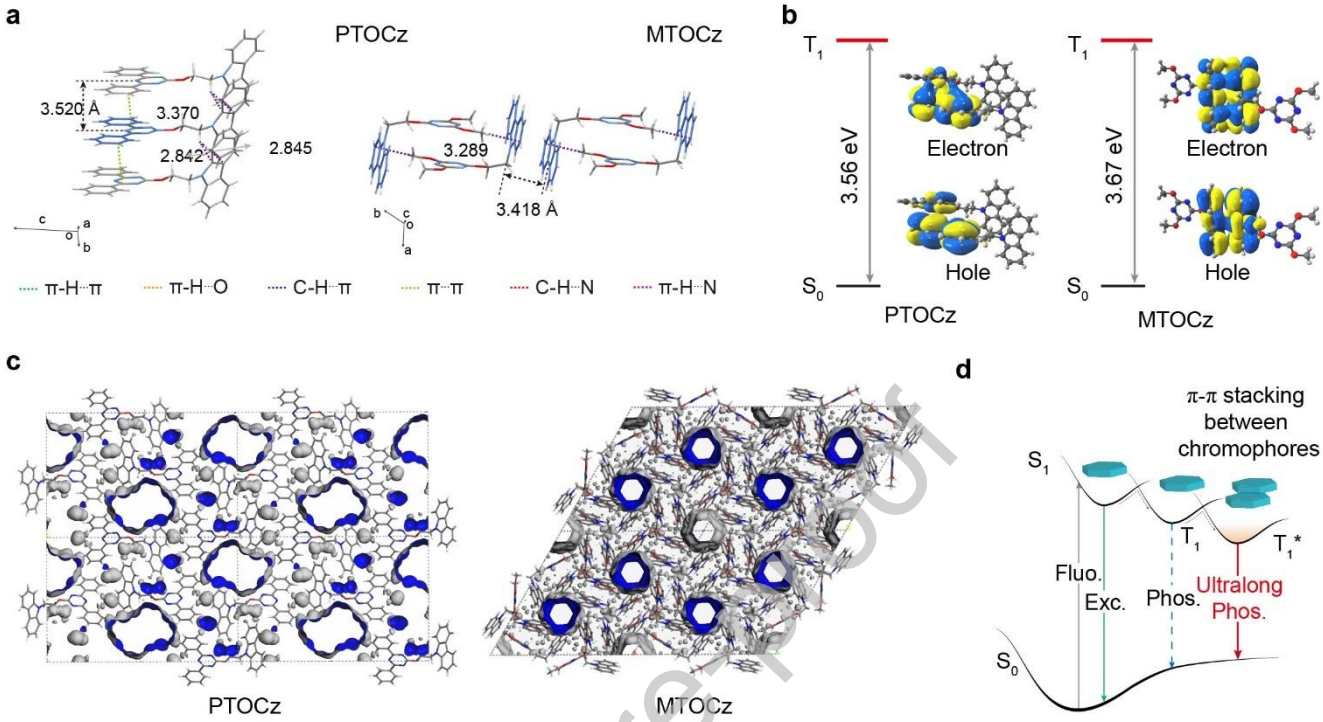

Fig. 4. Single crystal data of PTOCz and MTOCz crystals. (a) Intermolecular interactions between layer and column viewed from different axis in PTOCz and MTOCz crystal. (b) Natural transition orbitals (NTOs) for the lowest triplet state of molecular π-π stacking in PTOCz and MTOCz crystal. (c) The free volume region (cyan isosurface) in single crystal cells of PTOCz and MTOCz. (d) The deduced mechanism for the generation of ultralong organic phosphorescence in SOFs.

3.3 Proposed Mechanism for SOFs with Ultralong Phosphorescence Emission

To further probe the underlying mechanism of the observed ultralong organic phosphorescence from these SOFs, single crystal analysis and theoretical simulations were investigated (Fig. 4, S15-S18, Table S3-S5). Firstly, both PTOCz and MTOCz molecules have been fixed by multiple intermolecular and intramolecular interactions including hydrogen bonding, π…π interactions and so on. The highly twisted molecules in PTOCz and MTOCz can be efficiently limited by abundant intramolecular hydrogen bonds (2.445-2.890 Å) (Fig. 4a and 4b). These hydrogen bonds evenly distributed across the whole molecule to strongly confine molecular conformation.

As shown in Fig. 4a, the single molecule of PTOCz in their crystal lattice has restricted by adjacent two molecules in a column as well as in adjacent column also, mainly through C-H…π (2.842 Å and 2.845 Å), π…π (3.370 Å), π-H…π (2.893 Å) and π-H…N (2.671 Å). Two molecules in adjacent column linked with each other form an interlocked molecular dimer. These dimers were staggered with other dimer and extended into three dimensions to generate porous structures. In addition, adjacent molecules in a column displayed strong π-π stacking between the triazine parts having a distance of 3.520 Å. Thus, a rectangular hole for PTOCz was formed due to its various intermolecular interactions. In MTOCz, a 3D-stereo molecule was interlocked with its neighbouring molecules by C-H…π (3.289 Å) interactions. Two adjacent pairs of interlocked molecules in the same layer have connected by only strong π-π stacking between the carbazole groups with distance of 3.418 Å without any other interactions. The MTOCz molecule was also restricted by several types of intermolecular interactions, including C-H…N (2.685 Å) and π-H…O (2.709 Å) with two contiguous molecules in different layers along to c axis (Fig. 4b). Thus, multiple interactions lead to the generation of hexagonal holes of MTOCz. The porous structures for both crystalline materials were further verified by the stimulated free volume distribution in crystal (Fig 4c). The free volume in PTOCz and MTOCz crystals are 585.99 $Å^3$ and 1406.98 $Å^3$ (Table S4), respectively.

Moreover, taking the π-π stacking dimers of PTOCz and MTOCz crystals as the calculated models, it is easily found that the natural transition orbitals (NTOs) of the lowest triplet state (T_1) in PTOCz dimers were mainly distributed on triazines and their connected benzene groups, but those of MTOCz dimers were mainly located on carbazole groups (Fig. 4d and S18). In spite of their different phosphorescence chromophores, the energy level of T_1 state of PTOCz and MTOCz were similar (Table S5), which is consistent with earlier mentioned phosphorescence spectra. These results demonstrated that the phosphorescent chromophore of PTOCz molecules was triazine and benzene units, while that of MTOCz was carbazole. In a word, it has noted that phosphorescent chromophores in two SOFs all displayed fine π-π stacking. Thus, it was suggested that the effective π-π interactions between phosphorescent chromophores and hydrogen bonding restriction played critical roles in generating UOP features for SOFs by stabilizing triplet excitons (Fig. 4d).

4. Conclusions

In conclusion, we have designed and synthesized two SOFs, namely, PTOCz and MTOCz by introducing the alkyl chain into a densely packed planar molecule, to generate porosity. The crystals of both SOFs were prepared from the same solvent (di-chloromethane) at 25°C and both crystals have orange UOP. Surprisingly, we have found that PTOCz showed the longest phosphorescence lifetime of 762.56 ms in the reported porous materials. The crystal packing analyses demonstrate that the introduction of alkoxyl chain has promoted short-range π-π stacking to generate pores in crystal. Thus, we reasoned that the flexible alkoxyl chain played a significant role in the formation of SOFs. Combined the theoretical calculations, it is suggested that the phosphorescence emission of two compounds was mainly caused by the strong π-π stacking between their phosphorescence chromophores. Various interactions along with strong π-π stacking effectively fixed the molecular frameworks to suppress non-radiative decay and stabilized triplet excitons for UOP. This work will provide a platform to rationally design SOFs with ultralong phosphorescence.

Conflicts of interest

There are no conflicts to declare.

ACKNOWLEDGMENT

This work is supported by the National Natural Science Foundation of China (21975120, 9183304, 51673095, 61505078, 61935017 and 91833302), Natural Science Fund for Distinguished Young Scholars of Jiangsu Province (BK20180037), Projects of International Cooperation and Exchanges NSFC (51811530018). We are grateful to the High-Performance Computing Center of Nanjing Tech University for supporting the computational resources.

Notes and references

[1] W. Lustig, S. Mukherjee, N. Rudd, A. Desai, Li, S. Ghosh, Metal-Organic Frameworks: Functional Luminescent and Photonic Materials for Sensing Applications, Chem. Soc. Rev. 46 (2017) 3242-3285.

[2] Z. Dou, J. Yu, Y. Cui, Y. Yang, Z. Wang, D. Yang, G. Qian, Luminescent Metal-Organic Framework Films as Highly Sensitive and Fast-Response Oxygen Sensors. J. Am. Chem. Soc. 136 (2014) 5527-5530.

[3] Z. Hu, B. Deibert, J. Li, Luminescent Metal-Organic Frameworks for Chemical Sensing and Explosive Detection. Chem. Soc. Rev. 43 (2014) 5815-584.

[4] Y. Zhu, M. Qiao, W. Peng, Y. Li, G. Zhang, F. Zhang, Y. Li, X. Fan, Rapid Exfoliation of Layered Covalent Triazine-based Frameworks into N-doped Quantum Dots for the Selective Detection of Hg^{2+} Ions. J Mater. Chem. A 5 (2017) 9272-9278.

[5] W. Liu, X. Luo, Y. Bao, Y. Liu, G. Ning, I. Abdelwahab, L. Li, C. Nai, Z. Hu, D. Zhao, B. Liu, S. Quek, K. Loh, Two-Dimensional Conjugated Aromatic Polymer via C-C Coupling Reaction. Nat. Chem. 9 (2017) 563-570.

[6] W. Yang, A. Greenaway, X. Lin, R. Matsuda, A. J. Blake, C. Wilson, W. Lewis, P. Hubberstey, S. Kitagawa, N. R. Champness, M. Schröder, Exceptional Thermal Stability in a Supramolecular Organic Framework: Porosity and Gas Storage. J. Am. Chem. Soc. 132 (2010) 14457-14469.

[7] L. Tan, H. Li, Y. Tao, S. X. Zhang, B. Wang, Y. Yang, Pillar[5]arene‐Based Supramolecular Organic Frameworks for Highly Selective CO_2-Capture at Ambient Conditions. Adv. Mater. 26 (2014) 7027-7031.

[8] S. Dalapati, E. Jin, M. Addicoat, T. Heine, D. Jiang, Highly Emissive Covalent Organic Frameworks. J. Am. Chem. Soc. 138 (2016) 5797-5800.

[9] J. Dong, A. Tummanapelli, X. Li, S. Ying, H. Hirao, D. Zhao, Fluorescent Porous Organic Frameworks Containing Molecular Rotors for Size-Selective Recognition. Chem. Mater. 28 (2016) 7889-7897.

[10] J. Lü, C. Perez-Krap, M. Suyetin, N. H. Alsmail, Y. Yan, S. Yang, W. Lewis, E. Bichoutskaia, C. C. Tang, A. J. Blake, R. Cao, M. Schröder, A Robust Binary Supramolecular Organic Framework (SOF) with High CO_2 Adsorption and Selectivity. J. Am. Chem. Soc. 136 (2014) 12828-12831.

[11] Z. Li, Y. Zhang, H. Xia, Y. Mu, X. Liu, A Robust and Luminescent Covalent Organic Framework as a Highly Sensitive and Selective Sensor for the Detection of Cu2+ Ions. Chem. Commun. 52 (2016) 6613-6616.

[12] G. Lin, H. Ding, D. Yuan, B. Wang, C. Wang, A Pyrene-Based, Fluorescent Three-Dimensional Covalent Organic Framework. J. Am. Chem. Soc. 138 (2016) 3302-3305.

[13] M. Park, H. Kim, J. Murray, J. Koo, K. Kim, A Facile Preparation Method for Nanosized MOFs as a Multifunctional Material for Cellular Imaging and Drug Delivery. Supramol. Chem. 29 (2017) 441-445.

[14] X. Gao, Y. Wang, G. Ji, R. Cui, Z. Liu, One-Pot Synthesis of Hierarchical-Pore Metal-Organic Frameworks for Drug Delivery and Fluorescent Imaging. Cryst. Eng. Comm, 20 (2018) 1087-1093.

[15] K. Taylor, W. Rieter, W. Lin, Manganese-Based Nanoscale Metal-Organic Frameworks for Magnetic Resonance Imaging. J. Am. Chem. Soc. 130 (2008) 14358-14359.

[16] Y. Li, Y. Dong, X. Miao, Y. Ren, B. Zhang, P. Wang, Y. Yu, B. Li, L. Isaacs, L. Cao, Shape-Controllable and Fluorescent Supramolecular Organic Frameworks Through Aqueous Host-Guest Complexation. Angew. Chem., Int. Ed. 57 (2018) 729-733.

[17] J. Crowe, L. Baldwin, P. McGrier, Luminescent Covalent Organic Frameworks Containing a Homogeneous and Heterogeneous Distribution of Dehydrobenzoannulene Vertex Units. J. Am. Chem. Soc. 138 (2016) 10120-10123.

[18] M. Wang, S. Guo, Y. Li, L. Cai, J. Zou, G. Xu, W. Zhou, F. Zheng, G. Guo, A Direct White-Light-Emitting Metal-Organic Framework with Tunable Yellow-to-White Photoluminescence by Variation of Excitation Light. J. Am. Chem. Soc. 131 (2009) 13572-13573.

[19] J. Yu, Y. Cui, C. Wu, Y. Yang, B. Chen, G. Qian, Two-Photon Responsive Metal-Organic Framework. J. Am. Chem. Soc. 137 (2015) 4026-4029.

[20] Y. Cui, Y. Yue, G. Qian, B. Chen, Luminescent Functional Metal-Organic Frameworks. Chem. Rev. 112 (2011) 1126-1162.

[21] S. Wan, J. Guo, J. Kim, H. Ihee, D. Jiang, A Belt-Shaped, Blue Luminescent, and Semiconducting Covalent Organic Framework. Angew. Chem., Int. Ed. 47 (2008) 8826-8830.

[22] R. Xue, H. Guo, T. Wang, L. Gong, Y. Wang, J. Ai, D. Huang, H. Chen, W. Yang, Fluorescence Properties and Analytical Applications of Covalent Organic Frameworks. Anal. Methods 9 (2017) 3737-3350.

[23] X. Yang, D. Yan, Strongly Enhanced Long-Lived Persistent Room Temperature Phosphorescence Based on the Formation of Metal-Organic Hybrids. Adv. Opt. Mater. 4 (2016) 897-905.

[24] H. Wang, H. Shi, W. Ye, X. Yao, Q. Wang, C. Dong, W. Jia, H. Ma, S. Cai, K. Huang, L. Fu, Y. Zhang, J. Zhi, L. Gu, Y. Zhao, Z. An, W. Huang, Amorphous Ionic Polymers with Color-Tunable Ultralong Organic Phosphorescence 58 (2020) 18776-18782.

[25] R. Pashazadeh, P. Pander, A. Bucinskas, P. Skabara, F. Dias, J. Grazulevicius, Chemx. An Iminodibenzyl–Quinoxaline–Iminodibenzyl Scaffold as a Mechanochromic and Dual Emitter: Donor and Bridge Effects on Optical Properties. Chem. Commun. 54 (2018) 13857-13860.

[26] D. Li, F. Lu, J. Wang, W. Hu, X. Cao, X. Ma, H. Tian, Amorphous Metal-Free Room-Temperature Phosphorescent Small Molecules with Multicolor Photoluminescence via a Host−Guest and Dual-Emission Strategy. J. Am. Chem. Soc. 140 (2018) 1916-1923.

[27] S. Cai, H. Shi, J. Li, L. Gu, Y. Ni, Z. Cheng, S. Wang, W. Xiong, L. Li, Z. An, W. Huang, Visible-Light-Excited Ultralong Organic Phosphorescence by Manipulating Intermolecular Interactions. Adv. Mater. 29 (2017) 1701244.

[28] H. Shi, L. Zou, K. Huang, H. Wang, C. Sun, S. Wang, H. Ma, Y. He, J. P. Wang, H. Yu, W. Yao, Z. An, Q. Zhao, W. Huang, A Highly Efficient Red Metal-free Organic Phosphor for Time-Resolved Luminescence Imaging and Photodynamic Therapy. ACS Appl. Mater. Inter. 11 (2019) 18103-18110.

[29] Z. An, C. Zheng, Y. Tao, R. Chen, H. Shi, T. Chen, Z. Wang, H. Li, R. Deng, X. Liu, W. Huang, Stabilizing Triplet Excited States for Ultralong Organic Phosphorescence. Nat. Mater. 14 (2015) 685-690.

[30] C. Lin, Y. Zhuang, W. Li, T. Zhou, R. Xie, Blue, Green, and Red Full-Color Ultralong Afterglow in Nitrogen-Doped Carbon Dots. Nanoscale 11 (2019) 6584-6590.

[31] Z. Cheng, H. Shi, H. Ma, L. Bian, Q. Wu, L. Gu, S. Cai, X. Wang, W. Xiong, Z. An, W. Huang, Ultralong Phosphorescence from Organic Ionic Crystals under Ambient Conditions. Angew. Chem., Int. Ed. 57 (2018) 678-682.
[32] Y. Li, M. Geceviciusa, R. Qiu, Long Persistent Phosphors-from Fundamentals to Applications. J. Chem. Soc. Rev. 45 (2016) 2090-2136.
[33] Q. Fu, J. Chen, C. Shi, D. Ma, Solution-Processed Small Molecules as Mixed Host for Highly Efficient Blue and White Phosphorescent Organic Light-Emitting Diodes. ACS Appl. Mater. Inter. 4 (2012) 6579-6586.
[34] Z. Yu, Y. Wu, L. Xiao, J. Chen, Q. Liao, J. Yao, H. Fu, Organic Phosphorescence Nanowire Lasers. J. Am. Chem. Soc. 139 (2017) 6376-6381.
[35] M. Gu, H. Shi, K. Ling, A. Lv, K. Huang, M. Singh, H. Wang, L Gu, W.Yao, Z. An, H. Ma, W. Huang, Polymorphism-Dependent Dynamic Ultralong Organic Phosphorescence. Research. 2020 (2020) 8183450.
[36] J. Wang, X. Gu, H. Ma, Q. Peng, X. Huang, X. Zheng, S. Sung, G. Shan, J. Lam, Z. Shuai,B. Tang, A Facile Strategy for Realizing Room Temperature Phosphorescence and Single Molecule White Light Emission. Nat. Commun. 9 (2018) 1-9.
[37] D. Li, X. Yang, D. Yan, Cluster-Based Metal−Organic Frameworks: Modulated Singlet-Triplet Excited States and Temperature-Responsive Phosphorescent Switch. ACS Appl. Mater. Inter. 10 (2018) 34377-34384.
[38] H. Mieno, R. Kabe, N. Notsuka, M. Allendorf, C. Adachi, Long-Lived Room-Temperature Phosphorescence of Coronene in Zeolitic Imidazolate Framework ZIF-8. Adv. Opt. Mater. 4 (2016) 1015-1021.
[39] S. Mukherjee, P. Thilagar, Recent Advances in Purely Organic Phosphorescent materials. Chem. Commun. 51 (2015) 10988-11003.
[40] D. Zhou, Y. Xu, R. Lin, Z. Mo, W. Zhang, J. Zhang, High-Symmetry Hydrogen-Bonded Organic Frameworks: Air Separation and Crystal-to-Crystal Structural Transformation. Chem. Commun. 52 (2016) 4991-4994.
[41] P. Li, Y. He, Y. Zhao, L. Weng, H. Wang, R. Krishna, H. Wu, W. Zhou, M. O'Keeffe, Y. Han, B. Chen, A Rod-Packing Microporous Hydrogen-Bonded Organic Framework for Highly Selective Separation of C_2H_2/CO_2 at Room Temperature. Angew. Chem. Int. Ed. 54 (2015) 574-577.
[42] Y. Lin, X. Jiang, S. Kim, S. Alahakoon, X. Hou, Z. Zhang, C. R. Thompson, Smaldone, C. Ke, An Elastic Hydrogen-Bonded Cross-Linked Organic Framework for Effective Iodine Capture in Water. J. Am. Chem. Soc. 139 (2017) 7172-7175.
[43] X. Luo, X. Jia, J. Deng, J. Zhong, H. Liu, K. Wang, D. Zhong, A Microporous Hydrogen-Bonded Organic Framework: Exceptional Stability and Highly Selective Adsorption of Gas and Liquid. J. Am. Chem. Soc. 135 (2013) 11684-11687.
[44] S. Cai, H. Shi, Z. Zhang, X. Wang, H. Ma, N. Gan, Q. Wu, Z. Cheng, K. Ling, M. Gu, C. Ma, L. Gu, Z. An, W. Huang, Hydrogen-Bonded Organic Aromatic Frameworks for Ultralong Phosphorescence by Intralayer π-π Interactions. Angew. Chem., Int. Ed. 57 (2018) 4005-4009.
[45] L. Gu, H. Shi, M. Gu, K. H. Ling, Ma, S. Cai, L. Song, C. Ma, H. Li, G. Xing, X. Hang, J. Li, Y. Gao, W. Yao, Z. Shuai, Z. An, X. Liu, W. Huang, Dynamic Ultralong Organic Phosphorescence by Photoactivation. Angew. Chem., Int. Ed. 57 (2018) 8425-8431.
[46] Y. Zhao, H. Chen, L. Yin, X. Cheng, W. Zhang, X. Zhu, Chirality Induction of Achiral Polydialkylfluorenes by Chiral Solvation: Odd-even and Side Chain Length Dependence. Polym. Chem. 9 (2018) 2295-2301.
[47] D. Dang, X. Wang, D. Wang, Z. Yang, D. Hao, Y. Xu, S. Zhang, L. Meng, Fluorescent Organic Nanoparticles Constructed by a Facile "Self-Isolation Enhanced Emission" Strategy for Cell Imaging. ACS Appl. Nano Mater. 1 (2018) 2324-2331.
[48] S. Zhang, L. Yao, Q. Peng, W. Li, Y. Pan, R. Xiao, Y. Gao, C. Gu, Z. Wang, P. Lu, F. Li, S. Su, B. Yang, Y. Ma, Achieving a Significantly Increased Efficiency in Nondoped Pure Blue Fluorescent OLED: A Quasi-Equivalent Hybridized Excited State. Adv. Funct. Mater. 25 (2015), 1755-1762.
[49] H. Naito, K. Nishino, Y. Morisaki, K. Tanaka, Y. Chujo, Solid-State Emission of the Anthracene-o-Carborane Dyad from the Twisted-Intramolecular Charge Transfer in the Crystalline State. Angew.Chem., Int. Ed. 56 (2016), 254-259.
[50] H. Qian, M. E. Cousins, E. H. Horak, A. Wakefield, M. D. Liptak, I. Aprahamian, Suppression of Kasha's rule as a mechanism for fluorescent molecular rotors and aggregation-induced emission. Nat. Chem. 9 (2017), 83-87.
[51] L. Gu, H. Shi, C. Miao, Q. Wu, Z. Cheng, S. Cai, M. Gu, C. Ma, W. Yao, Y. Gao, Z. An, W. Huang, Prolonging the Lifetime of Ultralong Organic Phosphorescence through Dihydrogen Bonding. J. Mater. Chem. C 6 (2018) 226-233.
[52] Ma, C.; H. Ma, K. Ling, R. Zheng, M. Gu, L. Song, Z. An, H. Shi, W. Huang, Insight into Chirality on Molecular Stacking for Tunable Ultralong Organic Phosphorescence. J. Mater. Chem. C 6 (2018) 10179-10183.